Data Analysis of Recent Warming Pattern in the Arctic

著者	Ohashi Masahiro, Tanaka H. L.
journal or publication title	SOLA
volume	6A
page range	1-4
year	2010-03
権利	(c) 2010 by the Meteorological Society of Japan
URL	http://hdl.handle.net/2241/113536

doi: doi:10.2151/sola.6A-001

Data Analysis of Recent Warming Pattern in the Arctic

Masahiro Ohashi[1] and H. L. Tanaka[2]

[1]Graduate School of Life and Environmental Sciences, University of Tsukuba, Tsukuba, Japan

[2]Center for Computational Sciences, University of Tsukuba, Tsukuba, Japan

Abstract

In this study, we investigate the mechanism of the arctic warming pattern in surface air temperature (SAT) and sea ice concentrations over the last two decades in comparison with global warming since the 1970s.

According to the analysis result, it is found that the patterns of SAT and sea ice before 1989 are mostly determined by the Arctic Oscillation (AO) in winter. In contrast, arctic warming patterns after 1989 are characterized by the intensification of the Beaufort High and the reduced sea-ice concentrations in summer induced by the positive ice-albedo feedback.

It is concluded that the arctic warming before 1989 especially in winter was explained by the positive trend of the AOI. Moreover the intensified Beaufort High and the drastic decrease of the sea ice concentrations in September after 1989 were associated with the recent negative trend of the AOI. Since the decadal variation of the AO is recognized as the natural variability of the global atmosphere, it is shown that both of decadal variabilities before and after 1989 in the Arctic can be mostly explained by the natural variability of the AO not by the external response due to the human activity.

1. Introduction

The climate change associated with recent global warming is most prominent in the Arctic and Subarctic. The Intergovernmental Panel on Climate Change (IPCC) models also exhibit the largest warming in the Arctic for the 21st century (IPCC 2007). The Arctic Oscillation (AO) is the most dominant atmospheric phenomenon in winter characterized as opposing atmospheric pressure patterns at northern middle and high latitudes (Thompson and Wallace 1998). When the AO Index (AOI) is positive (relatively low pressures over the polar cap and high pressures at middle latitudes), the surface air temperature (SAT) is warmer than normal over Siberia and Canada, and cooler around Greenland (Wallace and Thompson 2002). When the AOI is negative, signs of the patterns are all reversed. This SAT pattern associated with the positive AO was similar to the recent global warming pattern (Chapman and Walsh 1993). Thompson et al. (2000) indicated that about half of the global warming pattern is explained by the AO. In addition, sea ice concentrations are decreasing in the Arctic Ocean more rapidly than the predictions by most of the climate models (Stroeve et al. 2007). According to Rigor et al. (2002) and Rigor and Wallace (2004), the decreasing sea ice concentrations were the response to the high AOI. Hence, the AO has attracted more attention as a crucial factor in explaining global warming. Ohashi and Tanaka (2009) suggested that observed decadal variability of the AO can be mostly explained by the internal variability of the atmosphere, and that the observed arctic warming pattern is mostly understood as the natural variability associated with the AO.

However, the increasing trend of the AOI since 1970 has stopped over the last two decades, and the AOI began to deviate from the global warming trend (Overland and Wang 2005). Cohen and Barlow (2005) suggested that the large-scale features of the global warming trend over the last 30 years are unrelated to the AO. Meanwhile, Lindsay and Zhang (2005) indicated that the arctic climate system began to enter a new climate regime by the effect of an ice-albedo feedback triggered by the positive AO phase for 1989−1995. The paradox between the climate change and the Arctic Oscillation was seen also for 1920−1940 when the Arctic indicated another warming period. This early 20th century warming was explained by the intrinsic variability of the atmosphere and other components of the climate system (e.g., sea ice, ocean, and land processes), as noted by Bengtsson et al. (2004). However, there are still many unknown factors in the relationship between the arctic warming and the AO.

In this study, we analyze the arctic climate change patterns in SAT and sea ice, and investigate their mechanism over the last two decades when the positive trend of the AOI has stopped. In addition, we examine the contributions from the internal variability and the response to the external forcing in the arctic climate change.

Corresponding author: H. L. Tanaka, Center for Computational Sciences, University of Tsukuba, 1-1-1 Tennodai, Tsukuba, Ibaraki 305-8577, Japan. E-mail: tanaka@sakura.cc.tsukuba.ac.jp.

2. Data and method

The data used in this study are monthly mean sea-level pressure (SLP) and SAT of the National Center for Environmental Prediction (NCEP)/National Center for Atmospheric Research (NCAR) reanalysis dataset. We used also monthly SAT of HadCRUT3 observation dataset (Brohan et al. 2006) and monthly sea ice concentrations of HadISST observation dataset (Rayner et al. 2003) provided by the Met Office Hadley Centre. The period of these data is 1950−2008. We defined the AO as the first empirical orthogonal function (EOF-1) of the winter (DJF) mean SLP in the north of 20°N. And the intensity of the Beaufort High is defined as the mean SLP anomaly over Beaufort Sea area (73.75−81.25°N, 130−170°W).

In addition, we used monthly SLP, SAT and sea ice concentration data of typical 10 Atmosphere-Ocean General Circulation Model (AOGCM) outputs; CCCMA[1]−CGCM3.1 (T47), GFDL[2]−CM2.1, GISS[3]−AOM, IPSL[4]−CM4, MIROC[5]3.2 (Medres), MPI[6]−ECHAM5, MRI[7]−CGCM2.3.2, NCAR−CCSM3, NCAR−PCM, and UKMO[8]−HadCM3; used in the IPCC 4th Assessment Report (AR4). We selected the 10 AOGCMs in reference to our previous paper of Ohashi and Tanaka (2009). These data are delivered by the Program for Climate Model Diagnosis and Intercomparison. The control scenarios used in this study are the 20th Century Climate in Coupled Model (20C3M) for 1901−1999 and the Special Report on Emission Scenarios (SRES)-A1B, SRES-A2, SRES-B1 for 2001−2099.

One of the advantages using the IPCC-AR4 models is that we can separate the atmospheric variability into the internal variability induced by the nonlinearity of the internal dynamics and the response to the external forcing such as increased greenhouse gases, solar constant variation and volcanic impact. Some

[1]Canadian Centre for Climate Modeling and Analysis
[2]Geophysical Fluid Dynamics Laboratory (USA)
[3]Goddard Institute for Space Studies (USA)
[4]Institute Pierre Simon Laplace (France)
[5]Center for Climate System Research Model for Interdisciplinary Research on Climate (Japan)
[6]Max Planck Institute for Meteorology (Germany)
[7]Meteorological Research Institute (Japan)
[8]United Kingdom Meteorological Office, Hadley Centre

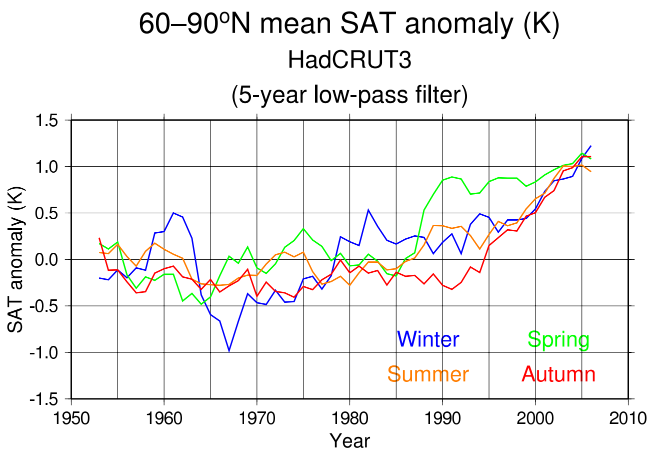

Fig. 1. Time series of the seasonal SAT anomaly in the Arctic (north of 60 °N). The blue, green, orange, and red lines represent winter, spring, summer, and autumn, respectively. The time series are the 5-year low-pass filtered.

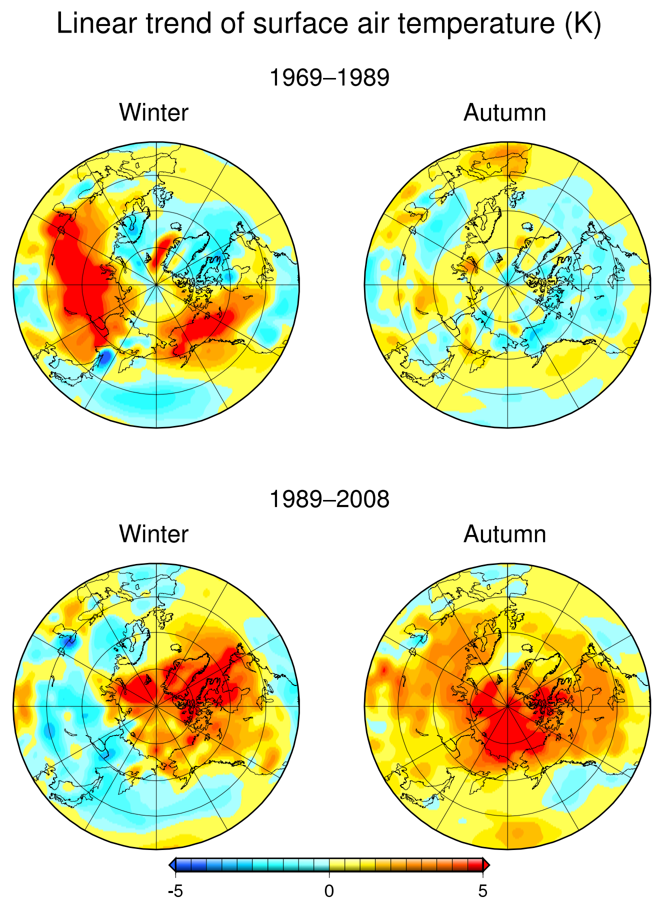

Fig. 2. Spatial distributions of linear trends of SAT in (left) winter and (right) autumn for (top) 1969−1989 and (bottom) 1989−2008 in north of 30°N.

AOGCMs used in IPCC-AR4 have ensemble members produced by integrations using the same external forcing but with slightly different initial data. Yukimoto and Kodera (2005) interpreted that the ensemble mean time series reflects the response to the external forcing, which is common to each ensemble member. In contrast, the deviations from the ensemble mean for each member are considered as internal variability. By this method, we calculated the ensemble means for MRI−CGCM2.3.2 outputs during the 21st century to evaluate the response to the external forcing for the AOI and the area mean SLP anomaly over the Beaufort Sea.

3. Results

Figure 1 shows time series of the seasonal SAT anomaly for 1951−2008 in the Arctic (north of 60°N). The blue, green, orange and red lines show the 5-year running mean of the time series for winter, spring, summer and autumn, respectively. As mentioned before, the arctic warming after 1970 to present is most prominent in winter. However, the arctic warming is more prominent in autumn than in winter over the last two decades since 1990. This rapid warming began when the positive trend of the AOI stopped. As is evident in autumn, the rapid warming may be related to the ice-albedo feedback of the arctic sea ice.

In addition, we compared the seasonal SAT patterns for 1989−2008 (the period when the AOI indicates a negative trend) with those for 1969−1989 (the period when the AOI indicates a positive trend). Figure 2 illustrates spatial distributions of linear trends of SAT in winter (DJF) and autumn (SON) during 1969−1989 and 1989−2008 in the north of 30°N. In 1969−1989, the spatial distribution in winter exhibits a positive AO pattern characterized as warming over Siberia and Canada, and cooling around Greenland. In autumn, the distribution is uniform showing almost no trend in SAT. Meanwhile, in 1989−2008, the arctic warming pattern in winter is characterized as the negative AO pattern showing cooling over Siberia and warming around Greenland. Note that, the warming pattern in autumn shows the largest warming over the Arctic Ocean suggesting the influence of the ice-albedo feedback. It may be important to note that the recent arctic warming for the last two decades is characterized by the ice-albedo pattern in autumn.

Using the EOF analysis, Teng et al. (2006) separated the 21st century SAT patterns simulated by NCAR−CCSM3 into the mode responding to the increase in radiative climate forcing and the mode related to the AO. Following this method, we analyzed next the winter SAT patterns associated with the AO in the late 20th century. Figure 3 shows spatial distributions of the EOF-1 and EOF-2 for winter mean SAT during 1951−1999 by NCEP/NCAR reanalysis and by the IPCC-AR4 10 AOGCM means for 20C3M. The SAT distribution of the EOF-1 (23.3%) for NCEP/NCAR reanalysis exhibits the typical AO pattern. However, the EOF-1 (32.7%) for IPCC Models shows the warming all over the Northern Hemisphere probably due to the ice-albedo feedback, which is not seen in the NCEP/NCAR reanalysis. It is found that the AO pattern appears in the EOF-2 (13.4%). The response to the external forcing as the common term for each model, appears as the most prominent mode. The SAT pattern associated with the AO is reduced in its variance by conducting the model mean. It is important to note that the AO, which is explained by the natural variability, must be dominant in the real atmosphere. This result supports the conclusion of Ohashi and Tanaka (2009).

Next, we analyzed the relationship between the sea ice concentrations in September and the surface pressure field because the SAT pattern in autumn over the last two decades is characterized by the ice-albedo pattern as shown in Fig. 2. Figure 4 illustrates spatial distributions of linear trends of sea ice concentrations in September for 1969−1989 and 1989−2008, and sea ice concentration anomaly in September regressed with the decadal AOI (the 11-year low-pass filtered AOI) and the mean SLP anomaly over Beaufort Sea in summer (JJA). The Beaufort High in summer is better correlated with sea ice in September than that in other seasons. Decreasing trend of sea ice in 1969−1989 is seen over the area near the Greenland Sea to the Kara Sea. This pattern is similar to the negative anomaly pattern of sea ice associated with the decadal AOI. Meanwhile, there is a remarkable sea ice decrease in the Beaufort, East Siberian and Chukchi Seas in 1989−2008. This pattern resembles the negative anomaly pattern of sea ice related

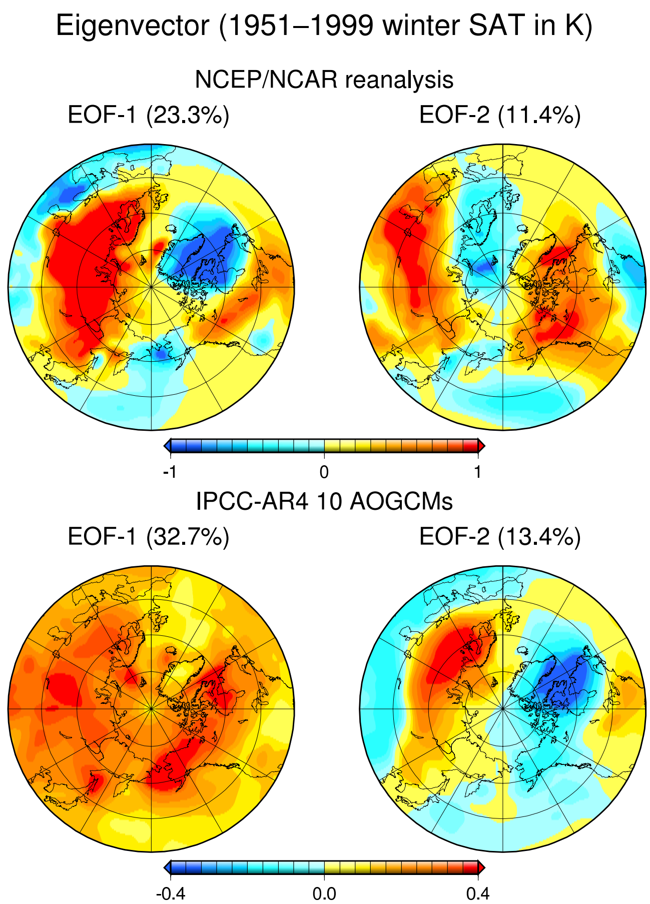

Fig. 3. Spatial distributions of (left) the EOF-1 and the (right) EOF-2 of the winter mean SAT for 1951−1999 by (top) NCEP/NCAR reanalysis and (bottom) IPCC-AR4 10 AOGCM means for 20C3M. Values in the parentheses show the contributions of the variance.

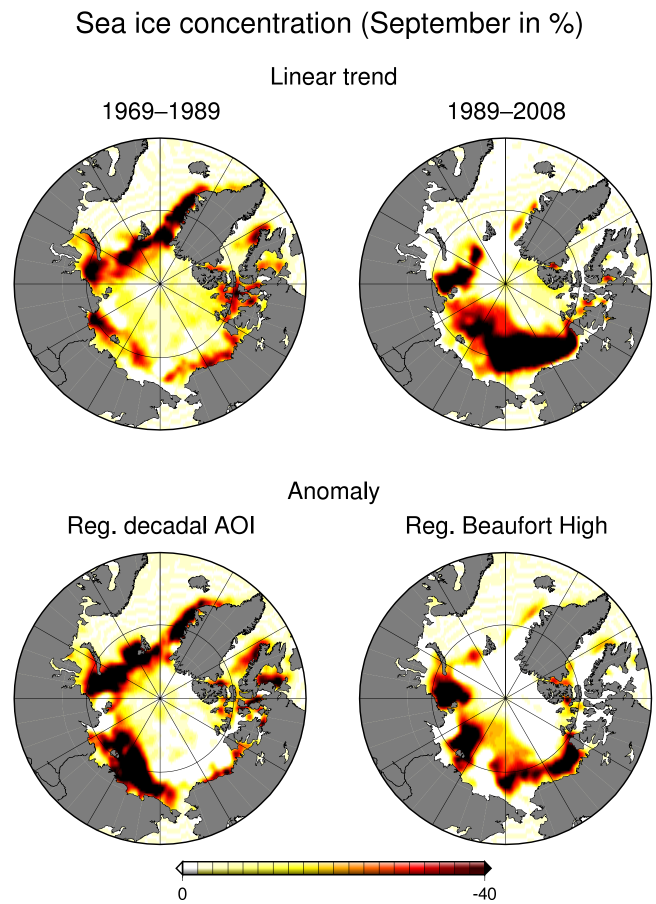

Fig. 4. Spatial distributions of (top) linear trends of sea ice concentration in September for (left) 1969−1989 and (right) 1989−2008, and (bottom) sea ice concentration anomalies in September regressed with (left) the decadal AOI and (right) the SLP anomaly over the Beaufort Sea in summer.

to the Beaufort High.

Finally, we examine the AOI and the intensity of the Beaufort High in the 21st century using ensemble runs of MRI−CGCM2.3.2. Figure 5 plots the time series of the AOI and the intensity of the Beaufort High in summer as the response to the external forcing for 2001−2099. The green, red and blue lines represent time series for SRES-A1B, SRES-A2 and SRES-B1, respectively. Although there is no trend in the AOI, the intensity of the Beaufort High tends to decrease with global warming. There is large amplitude of the internal variability, of course, as indicated by Ohashi and Tanaka (2009). The most important point in this result is that there is no difference between three SRES scenarios for the time series of both the AOI and the Beaufort High. This implies that the AO and the Beaufort High may vary without the human effects such as the increasing of greenhouse gases. However, it is not necessarily true that the Beaufort High varies without the anthropogenic influences, because the intensity of the Beaufort High tends to decrease with global warming.

4. Summary and discussions

The arctic warming in 1969−1989 can be explained mostly by the winter SAT pattern related to the positive trend of the AOI. In addition, the decrease of sea ice over the area near the Greenland Sea to the Kara Sea in this period is a result of the decadal variability of the AO. On the other hand, as the positive AOI trend shifts to negative since 1989, the Beaufort High has been intensified throughout the year. The intensified Beaufort High in summer tends to transport more ice toward Greenland, reducing the sea ice concentrations over the Beaufort Sea in September. By means of the ice-albedo feedback, the SAT in autumn has increased prominently. This ice-albedo feedback pattern was not seen in 1969−1989. The arctic warming before 1989 especially in winter was explained by the positive trend of the AOI. Moreover the intensified Beaufort High and the drastic decrease of the sea ice concentrations in September after 1989 were associated with the recent negative trend of the AOI. It should be noted that the intensity of the Beaufort High and sea ice change may interact with each other because the sea ice thickness relates closely to the variability of the Beaufort High.

We also analyzed the winter SAT pattern related to the AO in the late 20th century. It is very important to mention that there is no SAT pattern in the observation for the 20th century responded to the external forcing as shown by the EOF-1 of IPCC-AR4 models. The most dominant mode in the observation is the AO pattern, whereas the most dominant pattern is the ice-albedo pattern in the model. The winter SAT pattern observed in the late 20th century is not the response to the external forcing, but the natural variability related to the AO. Moreover, we compared three SRES scenarios of IPCC-AR4 model simulations in the 21st century to investigate anthropogenic influences against the AO and the Beaufort High. As a result, there are no differences between the SRES scenarios for both the time series of the AOI and the Beaufort High intensity. It was suggested that both time series vary without the human effects such as the increasing greenhouse gases in the 21st century. Since the AO and the Beaufort High in the Arctic may be the

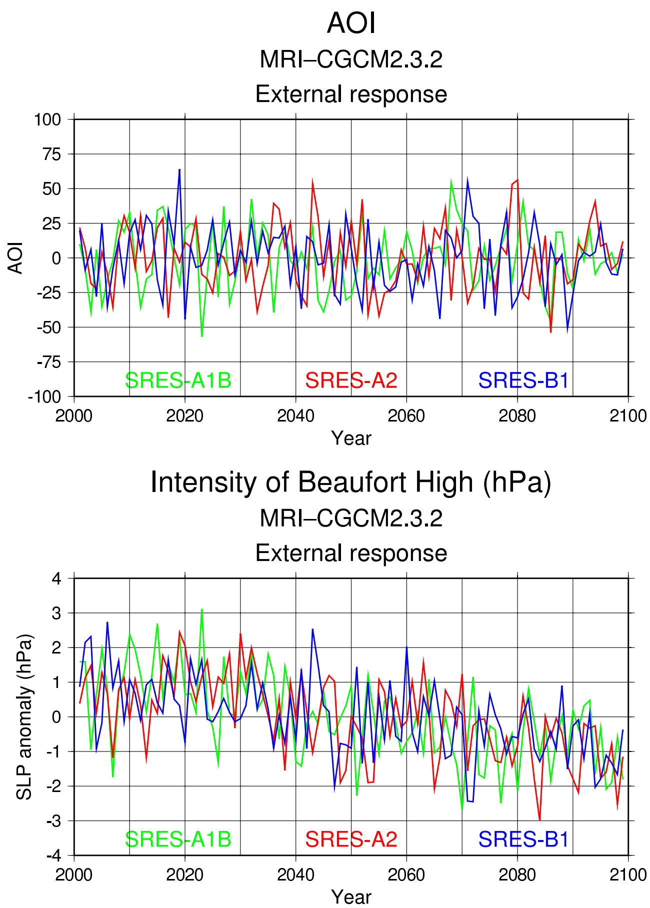

Fig. 5. Time series of (top) the AOI and (bottom) the intensity of the Beaufort High in summer as the response to the external forcing for 2001−2099 by MRI−CGCM2.3.2. The green, red, and blue lines represent SRES-A1B, SRES-A2 and SRES-B1, respectively.

stochastic natural variability in the atmospheric pressure field, the decreasing trend of sea ice in the Arctic may not be irreversible.

Acknowledgments

The authors would like to express acknowledgments to Dr. M. Matsueda of the MRI, Dr. K. Terasaki and Mr. K. Kondo of the University of Tsukuba for their technical support of the computer. We are grateful to the members of our Meteorology and Climatology group at the University of Tsukuba for their valuable comments.

References

Bengtsson, L., V. A. Semenov, and O. M. Johannessen, 2004: The early twentieth-century warming in the Arctic—A possible mechanism. *J. Climate*, **17**, 4045−4057.

Brohan, P., J. J. Kennedy, I. Harris, S. F. B. Tett, and P. D. Jones, 2006: Uncertainty estimates in regional and global observed temperature changes: A new dataset from 1850. *J. Geophys. Res.*, **111**, D12106, doi:10.1029/2005JD006548.

Chapman, W. L., and J. E. Walsh, 1993: Recent variations of sea ice and air temperature in high latitudes. *Bull. Amer. Meteor. Soc.*, **74**, 33−47.

Cohen, J., and M. Barlow, 2005: The NAO, the AO, and global warming: How closely related? *J. Climate*, **18**, 4498−4513.

Intergovernmental Panel on Climate Change, 2007: *Climate Change 2007: The Physical Science Basis*. Contribution of Working Group to the Fourth Assessment Report of the Intergovernmental Panel on Climate Change, Cambridge Univ. Press, 966 pp.

Lindsay, R. W., and J. Zhang, 2005: The thinning of Arctic sea ice, 1988−2003: Have we passed a tipping point? *J. Climate*, **18**, 4879−4894.

Ohashi, M., and H. L. Tanaka, 2009: Data analysis of Arctic Oscillation simulated by global warming prediction models. *Tenki*, **56**, 743−753, (in Japanese).

Overland, J. E., and M. Wang, 2005: The Arctic climate paradox: The recent decrease of the Arctic Oscillation. *Geophys. Res. Lett.*, **32**, L06701, doi:10.1029/2004GL21752.

Rayner, N. A., D. E. Parker, E. B. Horton, C. K. Folland, L. V. Alexander, D. P. Rowell, E. C. Kent, and A. Kaplan, 2003: Global analysis of sea surface temperature, sea ice, and night marine air temperature since the late nineteenth century. *J. Geophys. Res.*, **108**, D14, 4407, doi:10.1029/2002JD002670.

Rigor, I. G., and J. M. Wallace, 2004: Variations in the age of Arctic sea-ice and summer sea-ice extent. *Geophys. Res. Lett.*, **31**, L09401, doi:10.1029/2004GL19492.

Rigor, I. G., J. M. Wallace, and R. L. Colony, 2002: Response of sea ice to the Arctic Oscillation. *J. Climate*, **15**, 2648−2663.

Stroeve, J., M. M. Holland, W. Meier, T. Scambos, and M. Serreze, 2007: Arctic sea ice decline: Faster than forecast. *Geophys. Res. Lett.*, **34**, L09501, doi:10.1029/2007GL029703.

Teng, H., W. M. Washington, G. A. Meehl, L. E. Buja, and G. W. Strand, 2006a: Twenty-first century Arctic climate change in the CCSM3 IPCC scenario simulations. *Clim. Dyn.*, **26**, 601−616.

Thompson, D. W. J., and J. M. Wallace, 1998: The Arctic Oscillation signature in the wintertime geopotential height and temperature fields. *Geophys. Res. Lett.*, **25**, 1297−1300.

Thompson, D. W. J., J. M. Wallace, and G. Hegerl, 2000: Annular modes in the extratropical circulation Part II: Trends. *J. Climate*, **13**, 1018−1036.

Wallace, J. M., and D. W. J. Thompson, 2002: Annular modes and climate prediction. *Phys. Today*, **55**, 28−33.

Yukimoto, S., A. Noda, S. Uchiyama, T. Kusunoki, and A. Kitoh, 2006: Climate change of the twentieth trough twenty-first centuries simulated by the MRI-CGCM2.3. *Pap. Meteor. Geophys.*, **56**, 9−24.

Manuscript received 15 January 2010, accepted 23 February 2010
SOLA: http://www.jstage.jst.go.jp/browse/sola/